Progress In Electromagnetics Research B, Vol. 9, 137–149, 2008

A NOVEL DUALBAND FREQUENCY SELECTIVE SURFACE WITH PERIODIC CELL PERTURBATION

C. Guo, H. Sun, and X. Lu

Department of Electronic Engineering
School of Information Science and Technology
Beijing Institute of Technology
Beijing 100081, China

Abstract—A novel dualband frequency selective surface (FSS) with both a dielectric substrate and superstrate constructed by double-four-legged loaded slots (DFLLSs) is investigated, in which each periodic cell consists of two neighboring DFLLSs with different dimensions, its resonant frequencies occur at 183 GHz and 220 GHz. Good selectivity performance can be easily achieved both in lower passband and higher passband by tuning the dimensions of the DFLLSs. Besides, the passbands are mainly determined by the neighboring perturb cells and can be designed independently. According to the explicit physical concept and some formulas, the design process become straightforward and simple. Its frequency performance is obtained by using numerical simulation software CST based on finite difference time domain method (FDTD). The simulated results show the good stability of the resonant frequencies and bandwidths at different polarization states and various incident angles.

1. INTRODUCTION

Frequency selective surfaces (FSSs) are some periodic surfaces, which are basically assembly of identical elements arranged in one- or two-dimensional infinite arrays but finite arrays in practice [1]. FSSs find widespread applications as filters for microwaves and optical signals, have gained more an more attentions in recent years. The application of frequency selective surfaces are many and varied, they range over much of the electromagnetic spectrum. In the microwave region, for example, the frequency selective properties of FSS are exploited to make a reflector antenna more efficient, another typical application in this wavelength range is radome design. In the far-infrared region,

periodic screens are used as polarizers, beam splitters, as well as mirrors for improving the pumping efficiency in molecular lasers. In the near-infrared and visible portions of the spectrum, periodic screens have been proposed as solar selective surfaces to aid in the collection of solar energy [2]. Many of element shapes such as jerusalem cross and methods are proposed in other papers [3–12].

FSSs have been proven as a method to increase the capabilities of satellite communications when requirement of data communication links over multiple frequency bands makes it necessary to design a FSS operating at multiband frequencies. In space missions such as Voyager, Galileo, and Cassini, the use of dual-reflector antennas with a subreflection made of an FSS has made it possible to share the main reflector among different frequency bands [13–17].

Usually, one or the combination of several of the following techniques (see Fig. 1) are applied to the design of complex multiband FSSs: layered or stacked FSS, perturbation of a single-layered FSS, or multiresonant elements such as the double square loops or the

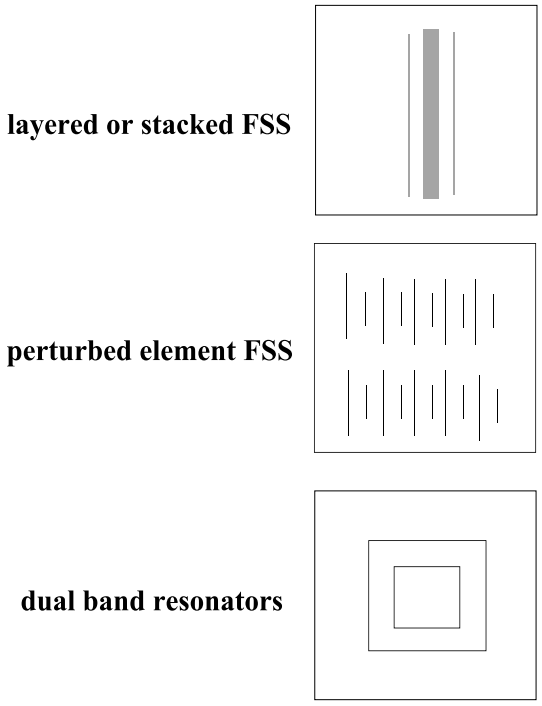

Figure 1. Several dualband FSS configurations [19].

concentric rings. The Cassini FSS is an example of a complex structure where two single-layer FSS with multiresonant elements are stacked to obtain the desired performance. However, for a lighter structure and the simplified design, using multiresonant elements is better choice [18].

In this paper, double-four-legged loaded slots (DFLLSs) [19] is adopted as dual band FSS element configuration. The shape of this FSS has self-similarity property. Self-similarity can be described as the replication of the geometry of the structure at a different scale within the same structure [8]. This paper presents the numerical simulated results of FSS with periodic cell perturbation, including the frequency response of the DF-LLS for the different polarizations, different incident angles. The main limitation to design a truly multiband FSS is the small band separation. Compared with combining conventional double concentric DFLLS, using the FSS with periodic cell perturbation can easily obtained the small band separation because the performance of the lower passband is easier to control. Thus the coupling between two self-similarity cells can be efficiently weakened.

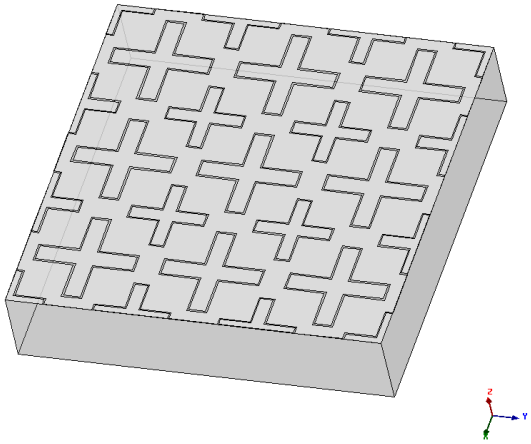

Figure 2. 3D model of the dualband FSS (the dielectric superstrate is hidden).

2. DESIGN

Figure 2 shows the 3D view of a part of dual band FSS, a cell is constructed by one big DFLLS in centre and four a quarter small DFLLSs in each corner of the square, and this cell is extended in the x and y direction infinitely. The top view of a cell's geometrical

configuration is shown in Fig. 3. Its detailed geometrical parameters are listed in Table 1, where ε_r, dh denote the permittivity, the thickness of the dielectric substrate and superstrate, respectively.

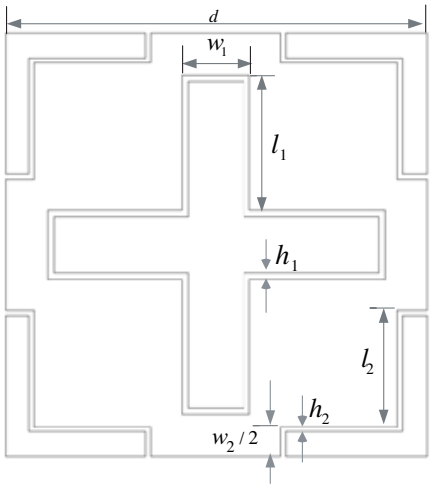

Figure 3. The top view of one cell of the DFLLSs.

Table 1. The geometrical parameters of DFLLS FSS used in the simulation.

l_1, mm	0.13	l_2, mm	l_1/k
w_1, mm	0.066	w_2, mm	w_1/k
h_1, mm	0.01	h_2, mm	h_1/k
dh, mm	0.254	tang (δ)	0.0009
ε_r	2.2	k	1.2

2.1. DFLLS Frequency Selective Surface

Following the early work of Munk [1], the development of the four-legged loaded elements is shown in Fig. 4. Although this paper mainly focuses on the research of the four-legged loaded slots elements, it is significant to have a plain recognition for the dipole element, because complementary arrays can be obtained by "Babinet's principle." However, the case is not adapted to the design in this paper, because the conducting screen is not a perfect conductor and "infinitely" thin. Besides, two layers of dielectric have been added, the resonant

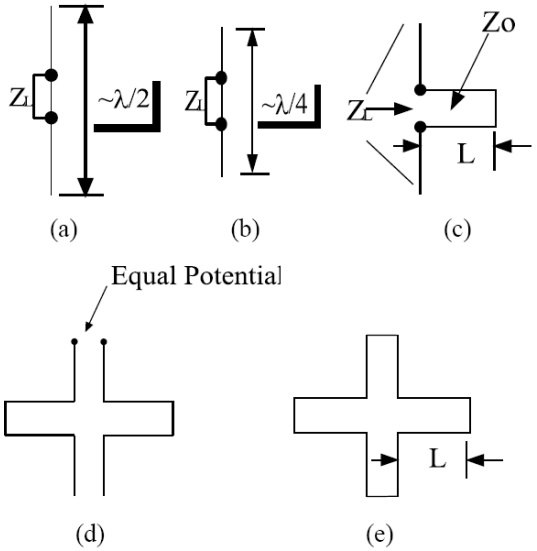

Figure 4. (a) Development of the four-legged loaded element starting from a simple $\lambda/2$ dipole. (b) That is shortened into a $\lambda/4$ dipole. (c) That is loaded with an inductive impedance in the form of a two wire transmission line. (d) Two elements are placed side by side to each other. (e) Since the potential of the tips of the two dipoles are the same, they can readily be connected and the four-legged loaded element is complete [1].

frequency will be shifted to a lower point somewhat for both the dipole and the slot arrays. From Fig. 4(a), this case can be considered as a simple $\lambda/2$ dipole antenna with load impedance Z_L under receiving condition; that is, its equivalent circuit is a generator connected to its radiation impedance $Z_A = R_A + jX_A$ in series with the load impedance Z_L. When $jX_A \sim 0$, resonant conditions is satisfied; that is, the strongest current can be obtained for $Z_L = 0$. Making an element smaller is usually useful to pack the elements closer together, resulting generally in better resonant stability with angle of incidence and possibly greater bandwidth [1]. Thus in Fig. 4(b), the total length of the dipole has been shortened to about $\lambda/4$, thereby changing the radiation impedance to $R_a - jX_a$, it is now strongly capacitive. However, choosing the load impedance to be inductive, $Z_L = +jX_a$, maximum current can be obtained and the resonant conditions can be satisfied. The practical execution of the load impedance Z_L is shown in Fig. 4(c), namely in the form of a two wire transmission line of length

$l \sim \lambda/8$ and characteristic impedance Z_0. In Fig. 4(d) two dipoles with loads have been placed next to each other, which primarily has the effect of cutting the effective load impedance in half. However, the tips of the two dipoles will have essentially the same potential; that is, a short can be freely added between them as illustrated in Fig. 4(e). The four-legged loaded element is complete.

The resonance of DFLLS occurs when the circumference of the four-legged element is a multiple of the wavelength. However, the resonant frequency changes to somewhere between f_0 and $f_0/\sqrt{\varepsilon_r}$ when a dielectric slab is added next to a periodic structure. Furthermore, the size of the big DFLLS can be obtained by multiply scale factor k and the size of small DFLLS. This paper adopt this element as the cell of dualband because this element can provide the narrow bandwidths compared with other elements such as the hexagon, besides, the four-legged loaded elements are capable of considerable variation by changing the elements themselves [1], with the exception of that, the another advantage is these elements can be easy to pack closer, which is important when designing the multiband FSS.

2.2. Dualband DFLLS FSS with Narrow Band Separation

In multiband FSS design, band separation is an important specification. In a conventional multiband constructed by concentric dipoles or slots, the band separation is proportional to the clearance between concentric elements. When narrow band separation is needed, the scale factor k should be small, resulting in the small clearance between concentric elements. Thus, this brings two problems, one is strict requirement for fabrication process, the other is some unexpected coupling between the concentric elements occur.

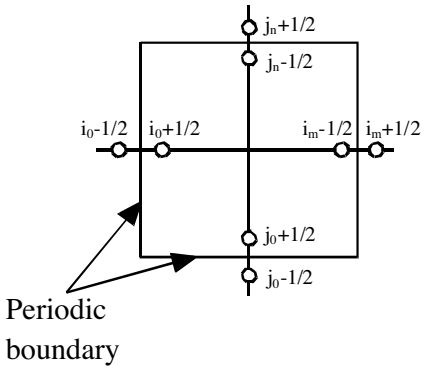

Figure 5. Periodic boundary in a unit of FSS.

These problems can be efficiently solved in multiband FSS design using neighboring perturbed DFLLSs as elements. The narrow band separation can be achieved by adjusting the scale factor k. This advantage decide the array arrangement.

2.3. Formulations

Many methods have been adopted to analyze the reflection and transmission characteristics of a FSS, such as PMoM, FEM, FDTD and spectral domain approach, etc. In this paper, FDTD method is adopted to calculate the transmission coefficients of the DFLLSs. The software CST based on this method are applied to analyze it, and we assume the whole FSS is an infinite periodic structure, so only one period unit need to be computed, other parameters can be obtained by Floquet boundary and absorbing boundary. The excitation can be set as a plane wave of arbitrary incident angle and arbitrary polarization.

The FDTD method is formulated by discretizing Maxwell's curl equations and approximating the derivatives with difference. The Maxwell's equation in difference fan can be referred to [17]. The Fig. 5 [17] shows a unit and periodic boundary, so the electric field and magnetic field formulations [17] at the mesh nodes on four periodic surfaces can be constructed by Floquet theorem [1] as

$$\begin{aligned}
\phi\left(i_m+\frac{1}{2}\right) &= \phi\left(i_0+\frac{1}{2}\right)e^{-jk\sin\theta\cos\varphi D_x}\\
\phi\left(i_0-\frac{1}{2}\right) &= \phi\left(i_m-\frac{1}{2}\right)e^{jk\sin\theta\cos\varphi D_x}\\
\phi\left(j_n+\frac{1}{2}\right) &= \phi\left(j_0+\frac{1}{2}\right)e^{-jk\sin\theta\cos\varphi D_y}\\
\phi\left(j_0-\frac{1}{2}\right) &= \phi\left(j_n-\frac{1}{2}\right)e^{jk\sin\theta\cos\varphi D_y}
\end{aligned} \tag{1}$$

The Mur's absorbing boundary condition (ABC) of second order is applied to truncate the computation domain at bottom and upper planes, the ABC formulation is written in [17].

Once the electric field distribution is obtained everywhere in the structure, the parameter of power transmission coefficient T of the DFLLS FSS is evaluated by using the following formulate:

$$T=\frac{P_z^t}{p_z^i}=\frac{\int\left(E_x^t\times H_y^{t^*}-E_y^t\times H_x^{t^*}\right)ds}{\int\left(E_x^i\times H_y^{i^*}-E_y^i\times H_x^{i^*}\right)ds}. \tag{2}$$

3. THE SIMULATED RESULTS

Electric field distribution diagrams at resonant frequencies for different polarization states are plotted in Fig. 6, it can be seen that four-legged loaded element actually works with "two legs" for both TE and TM polarizations. It can be explained that each leg exhibits transmission property for electric field vector those perpendicular to it, on the contrary, reflection property for electric field vector those tangential to it.

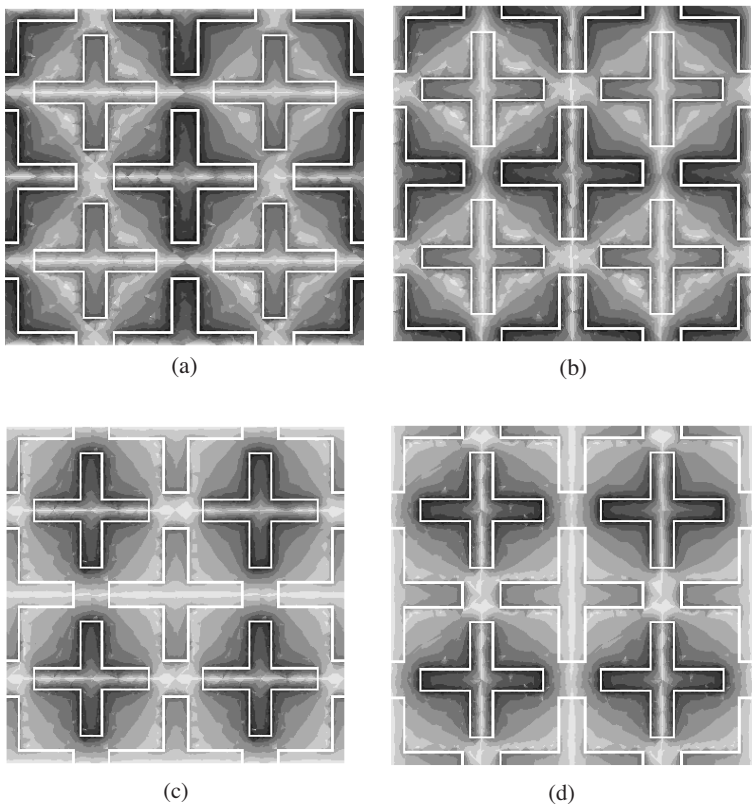

Figure 6. Electric field distribution diagrams at different frequencies with TE and TM polarizations when incident angle $\theta = 0°$. (a) 183 GHz, TE. (b) 183 GHz, TM. (c) 220 GHz, TE. (d) 220 GHz, TM.

Figure 7 shows the frequency response curve of the DFLLS FSS with different angles at TE and TM polarization when $k = 1.2$. In the range of 75 GHz to 300 GHz, the results show that resonant frequencies occur at 183.2 GHz and 219.7 GHz, that is, there are two

zeros respectively at 183.2 GHz and 219.7 GHz, and one pole between them at 204.01 GHz. In lower passband, the bandwidth of −0.5 dB and −3 dB are 21.17 GHz, 49.59 GHz respectively, while in higher passband, the corresponding values are 17.25 GHz and 43.65 GHz.

The zeros at 183.2 GHz and 219.7 GHz this type of FSS are caused

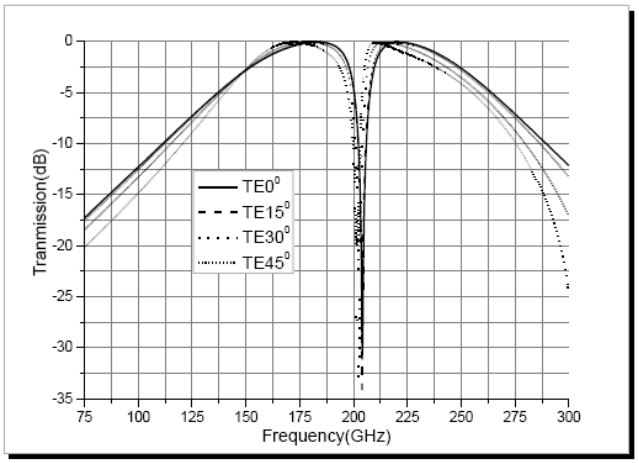

(a) TE

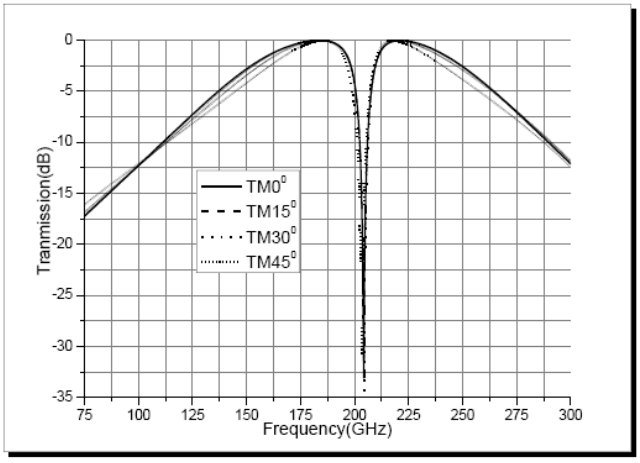

(b) TM

Figure 7. Transmission response of the DFLLS FSS with different incident angles at two polarization states when $k = 1.2$.

by the resonance of the neighboring periodic slots respectively. The pole at 204.01 GHz can be explained with Foster's reactance theorem that between two nulls will always be a pole. As the description as in Section 2, because of the symmetry of the structure, the frequency response curve has little changes with different polarization states at normal incidence. In addition, the curve keeps the approximate coherence with different incident angles at TE and TM polarization especially TM polarization. From the Fig. 7(a), it can be seen that the higher resonant frequency is pulled down a little with increase of the incident angle at TE polarization. In short, the simulated results show that the selectivity and bandwidth of the dual passband are insensitive to incident angles and polarization states.

The several parameters that have effects on FSS are the dimensions of four-legged loaded slot and interelement spacing, the dimensions of this FSS have been detailed described in [1] and [19]. This paper mainly focuses on the effect of interelement spacing on FSS. In the multiband FSS design, the grating lobes should be taken into account, grating lobes can't be avoid. However, when some conditions are meet, onset of grating lobes can be delayed [1]. When the needed high resonant frequency is approximate 2 times or more than low resonant frequency, interelement spacing d becomes important, onset of grating lobes can be controlled by adjusting d. Fig. 8 shows the

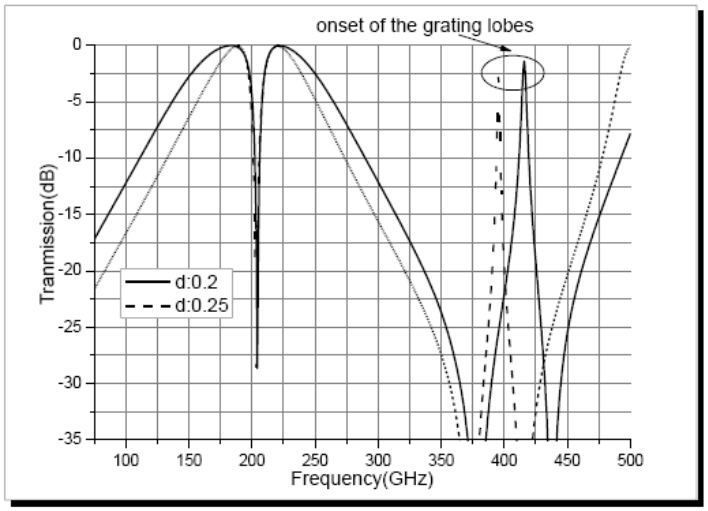

Figure 8. Frequency response of the DFLLS FSS with different interelement spacing at TM polarization, the incident angle θ is 0°.

frequency response of the DFLLS FSS with different interelement spacing d at TM polarization when the incident angle is 0°, with the decrease of the interelement spacing, the resonant frequency remains essentially constant while onset of the grating lobes caused by the outer slot is delayed, and the bandwidth increases considerably. Besides, compared with other types of FSSs, the advantage of this type of FSS is that the elements are easier to be packed close, that is, the array gets more densely packed, which makes the bandwidth larger and larger.

4. CONCLUSIONS

A dualband FSS with perturbed neighboring four-legged loaded slots elements has been investigated by numerical simulation. Design process including choice of element and array arrangement has been demonstrated. Its frequency performance has been analyzed in detail. The main parameters that affects frequency response have been discussed. The simulated results indicate that the DFLLS FSS remains constant of the resonant frequency and stability of the bandwidth at different polarization states and various incident angles, the other advantage of this type of FSS is that more compact array can be obtained, consequently, larger bandwidth have been achieved. Besides, narrow band spacing can be easily implemented. The RT/D 5880 are used as the substrate and superstrate, and this FSS could be accurately fabricated using optical contact lithography [20]. Another important factor shouldn't be ignored, that is, in practical application, it is necessary to placing the rigid foam on the two sides of FSS for protecting it, the permittivity of this material is close to 1, so it would not affect the performance of the FSS.

REFERENCES

1. Munk, B. A., *Frequency Selective Surfaces: Theory and Design*, Wiley-Interscience, New York, 2000.
2. Mittra, R., C. H. Chan, and T. Cwik, "Techniques for analyzing frequency selective surfaces-a review," *IEEE Proc.*, Vol. 76, No. 12, 1593–1615, 1988.
3. Ma, D. and W.-X. Zhang, "Mechanically tunable frequency selective surface with square-loop-slot elements," *Journal of Electromagnetic Waves and Applications*, Vol. 21, No. 15, 2267–2276, 2007.
4. Qing, A. and C. K. Lee, "An improved model for full wave analysis of multiplayered frequency selective surfaces with gridded square

element," *Progress In Electromagnetics Research*, PIER 30, 285–303, 2001.

5. Zheng, G., A. A. Kishk, A. W. Glisson, and A. B. Yakovlev, "Implementation of Mur's absorbing boundaries with periodic structures to speed up the design process using finite-difference time-domain method," *Progress In Electromagnetics Research*, PIER 58, 101–114, 2006.
6. Tang, W., X. He, T. Pan, and Y. L. Chow, "Synthetic asymptote formulas of equivalent circuit components of square spiral inductors," *Journal of Electromagnetic Waves and Applications*, Vol. 20, No. 2, 215–226, 2006.
7. Gu, Y.-Y., W.-X. Zhang, and Z.-C. Ge, "Two improved Fabry-Perot resonator printed antennas using EBG superstrate and AMC substrate," *Journal of Electromagnetic Waves and Applications*, Vol. 21, No. 6, 719–728, 2007.
8. Wu, C. and G.-X. Jiang, "Stabilization procedure for the time-domain integral equation," *Journal of Electromagnetic Waves and Applications*, Vol. 21, No. 11, 1507–1512, 2007.
9. Hosseini, M., A. Pirhadi, and M. Hakkak, "A novel AMC with little sensitivity to the angle of incidence using 2-layer Jerusalem cross FSS," *Progress In Electromagnetics Research*, PIER 64, 43–51, 2006.
10. Ho, M., "Scattering of electromagnetic waves from vibrating perfect surfaces: Simulation using relativistic boundary conditions," *Journal of Electromagnetic Waves and Applications*, Vol. 20, No. 4, 425–433, 2006.
11. Hosseini, M., A. Pirhadi, and M. Hakkak, "Design of a nonuniform high impedance surface for a low profile antenna," *Journal of ElectroMagnetics Waves and Applications*, Vol. 20, No. 11, 1455–1464, 2006.
12. Xiao, J.-K. and Y. Li, "Novel compact microstrip square ring bandpass filters," *Journal of Electromagnetic Waves and Applications*, Vol. 20, No. 13, 1817–1826, 2006.
13. Munk, B., R. Kouyoumjian, and L. Peters, Jr., "Reflection properties of periodic surfaces of loaded dipoles," *IEEE Trans. Antennas Propag.*, Vol. 19, 612–617, Sept. 1971.
14. Wu, T. K., "Four-band frequency selective surface with double square loop patch elements," *IEEE Trans. Antennas Propag.*, Vol. 42, No. 12, 1659–1663, 1994.
15. Wu, T. K. and S. W. Lee, "Multiband frequency surface with multiring patch elements," *IEEE Trans. Antennas Propag.*,

Vol. 42, No. 11, 1484–1490, 1994.

16. Huang, J., T. K. Wu, and S. W. Lee, "Tri-band frequency selective surface with circular ring elements," *IEEE Trans. Antennas Propag.*, Vol. 42, No. 2, 166–175, 1994.
17. Luo, G. Q., W. Hong, Z. C. Hao, B. Liu, W. D. Li, J. X. Chen, H. X. Zhou, and K. Wu, "Theory and experiment of novel frequency selective surface based on substrate integrated waveguide technology," *IEEE Trans. Antennas Propag.*, Vol. 53, No. 12, 4035–4043, 2005.
18. Romeu, J. and Y. Rahamat-Samii, "Fractal FSS: A novel dual-band frequency selective surface," *IEEE Trans. Antennas Propag.*, Vol. 48, No. 7, 1097–1105, 2000.
19. Guo, C., H. J. Sun, and X. Lu, "Dualband frequency selective surface with double-four-legged loaded slots elements," *Microwave and Millimeter Wave Technology, 2008. ICMMT 2008. International Conference*, Vol. 1, 297–300, April 21–24, 2008.
20. Bossard, J. A., D. H. Werner, T. S. Mayer, J. A. Smith, Y. U. Tang, R. P. Drupp, and L. Li, "The design and fabrication of planar multiband metallodielectric frequency selective surfaces for infrared applications," *IEEE Trans. Atennas Propag.*, Vol. 54, No. 4, 1265–1276, Apr. 2006.